Pattern Recognition Letters 8 (1988) 257–269
North-Holland

November 1988

A note on grey level–intensity transformation: effect on HVS thresholding

M.K. KUNDU and S.K. PAL

Electronics and Communication Sciences Unit, Indian Statistical Institute, 203 Barrackpore Trunk Road, Calcutta 700 035, India

Received 4 May 1988
Revised 26 July 1988

Abstract. An attempt is made in this note to investigate the effect on edge extraction when the theory of HVS (human visual system) based thresholding [1] is made to operate on the intensity domain of a grey tone image. A family of S and S^{-1} functions is considered to take care of the grey level to intensity transformation. The performance of the system is also quantitatively analysed using the measure 'entropy' of a fuzzy set.

Key words. HVS thresholding, edge extraction, grey level–intensity transformation.

Introduction

An algorithm for thresholding based on the facts human psychovisual phenomena or the response the human visual system (HVS) was reported in We call this method HVS based thresholding oughout this text. This made it possible to select omatically (without human intervention) the esholds for detecting the significant edges as per- ed by human beings. The threshold value apts the background intensity according to the ction governed by a characteristic of one of the Vries Rose, Weber and saturation regions. ese regions are characterised in the intensity do- ain by

$$\Delta B_t \propto \sqrt{B}, \tag{1a}$$

$$\Delta B_t \propto B, \quad \text{and} \tag{1b}$$

$$\Delta B_t \propto B^2, \tag{1c}$$

pectively. ΔB_t and B denote the incremental eshold and background intensity. Equation (1) presents HVS characteristics. The algorithms e found for a wide range of images to provide satisfactory improvement in the performance in conventional edge detection process.

It is to be noted that while implementing the above mentioned algorithms for a digital grey tone image, it was implicitly assumed that there exists a linear relation between the discrete intensity and grey level so that the intensity values can well be substituted by its corresponding transformed grey level values without affecting the above characteristic equations (1) of the HVS.

In practice, when scanning an image, there is a non-trivial transformation function which links intensities going in and grey scales coming out. The question may therefore arise (in fact, raised by many readers) how the results [1] will be affected if one considers the exact transformation used during the digitisation process.

A typical form of the response $C = f(B)$ between the digitised grey value (C) and the intensity value (B) (sensor input luminance value) is shown in Figures 1 [2]. The compensation methods to have a distortion free grey image are discussed in the literature [2].

An attempt is made in this letter to investigate the effect on the HVS based edge thresholding when a grey tone image undergoes an inverse transformation $B = f^{-1}(C)$ before taken as input. Different versions of S function [3] which closely resemble the response in Figure 1 have been considered. The

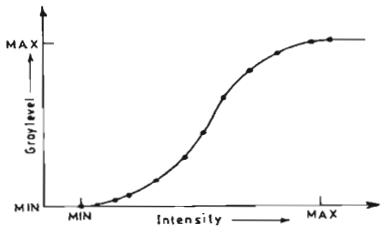

Figure 1. A typical intensity – grey level transformation [2].

concept of 'entropy of fuzzy subsets' [3, 4] is used as a tool for providing quantitative analysis of the results obtained.

2. HVS based edge extraction [1]

If we assume that the composite visual response curve representing De Vries–Rose, Weber and saturation regions could be represented by piecewise linear segments, then the characteristic equations for the different regions could be expressed as [1]:

$$\log \Delta B_T = \log B + \log k_1, \tag{2a}$$

$$\log \Delta B_T = \tfrac{1}{2} \log B + \log k_2, \tag{2b}$$

$$\log \Delta B_T = 2 \log B + \log k_3 \tag{2c}$$

where

$$k_1 = \tfrac{1}{100}\beta\left(\frac{\Delta B}{B}\right)_{max}$$

$$k_2 = k_1/\sqrt{B_{x_2}},$$

$$k_3 = k_1/B_{x_3},$$

where B_{x_2} and B_{x_3} are the upper- and lower-end background intensity values for the Weber region, and β is the constant representing characteristics of the Weber region.

The minimum amount of brightness (ΔB_T) by which the intensity of an object must be greater or less than its background intensity B in order to make the object appear brighter or darker is given by the following set of relations:

$$\Delta B_T = \frac{\sqrt{B}}{100}\beta\left(\frac{\Delta B}{B}\right)_{max}\sqrt{B_{x_2}}, \tag{3a}$$

$$B_{x_2} \geq B > B_{x_3},$$

B_{x_3} = absolute minimum visual threshold

$$= \frac{B}{100}\beta\left(\frac{\Delta B}{B}\right)_{max}, \quad B_{x_2} \geq B \geq B_{x_3}, \tag{3b}$$

$$= \frac{B^2}{100}\beta\left(\frac{\Delta B}{B}\right)_{max}\frac{1}{B_{x_3}}, \quad B \geq B_{x_3}. \tag{3c}$$

So if the intensity difference between the point under consideration and its background (ΔB_T) exceeds the minimum as expressed by the above equations under different background intensity conditions, then the point will be considered as detectable (valid) edge point.

3. S and S^{-1} functions

In order to generate a reasonably approximated version of the response curve in Figure 1, let us consider first of all the S-type function [3],

$$C = f(B) = \left[1 + \left(\frac{B_{max} - B}{F_d}\right)^{F_e}\right]^{-1} \tag{4}$$

which is widely used in the image processing problems. Here F_e and F_d are the positive constants which control the slope and spread of the enhancement function. Varying these parameters one can achieve any desired amount of enhancement. These are also termed as fuzzifiers when $C = f(B)$ represents an S-type membership function of a fuzzy set [3]. In that case they control the amount of fuzziness in the set. From equation (4) we see that C lies in the interval $[\alpha, 1]$ where

$$\alpha = \left[1 + \left(\frac{B_{max}}{F_d}\right)^{F_e}\right]^{-1} > 0. \tag{5}$$

α denotes the intercept on the C-axis. From eq. (4) we can generate another function (modified), such that

$$C = f_1(B) = \left[1 + \left(\frac{B_{max} - B}{F_d}\right)^{F_e}\right]^{-1} - 2\alpha \tag{6}$$

whose response is shown in Figure 2 for different

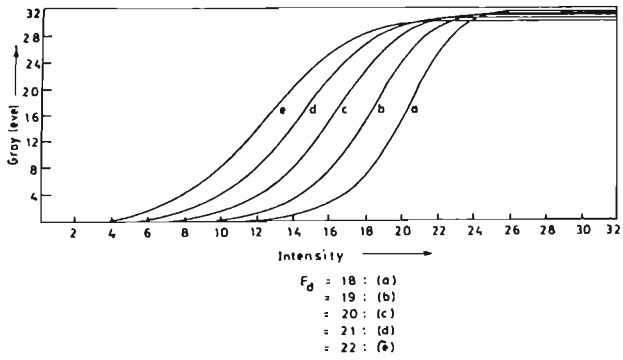

Figure 2. S-type functions.

lues of F_d with $F_c = 8$.

Thus Figure 2 has a close resemblance to Figure 1. is to be noted that C in eq. (6) lies in $[0, \alpha']$, $\alpha' < 1$, eing the value of C for which $B = B_{max}$. Therefore the inverse transformation

$$B = f_1^{-1}(C) \tag{7}$$

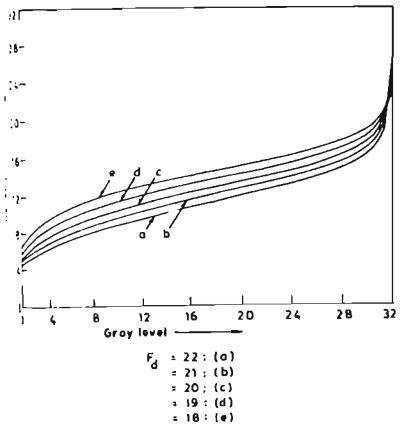

Figure 3. S^{-1}-type functions.

can be used to recover the discrete intensity value from its corresponding grey level value. A plot of eq. (7) is shown in Figure 3.

Now, the nonlinear form (Figure 2) for intensity-grey level transformation can also be viewed as a contrast enhancement function [3]. In other words, the digitisation procedure inherently introduces some enhancement in the image while transforming the intensity values to grey level. Therefore, the grey level–discrete intensity transformation (Figure 3) can be viewed as an operation which leads to reduction in dynamic range by compressing the levels in the middle region. Because of the compression in dynamic range, the entropy of the resulting image which denotes in a global sense, the average amount of difficulty (ambiguity) in deciding whether a pixel would be considered a member of the 'bright'/'dark' image will increase. Entropy of an image is defined in the following section.

4. Entropy of an image

Entropy of an $M \times N$ L-level image in the light of fuzzy set theory is defined as [3]:

$$H(X) = \frac{1}{MN \ln 2} \sum_m \sum_n S_n(\mu_X(x_{mn})) \tag{8}$$

with

$$S_n(\mu_X(x_{mn})) = -\mu_X(x_{mn}) \ln \mu_X(x_{mn}) - (1-\mu_X(x_{mn})) \ln(1-\mu_X(x_{mn})) \quad (9)$$
$$m = 1,2,\ldots,M, \quad n = 1,2,\ldots,N.$$

$\mu_X(x_{mn})$ $(1 \geq \mu_X(x_{mn}) \geq 0)$ denotes the grade of possessing some brightness property (defined by equation (12)) by the (m,n)th pixel intensity x_{mn}.

$H(X)$ has the following properties:

$$H(X) = 0 \text{ (minimum) for } \mu_X(x_{mn}) = 0 \text{ or } 1 \ \forall(m,n). \quad (10a)$$

$$H(X) = 1 \text{ (maximum) for } \mu_X(x_{mn}) = 0.5 \ \forall(m,n). \quad (10b)$$

$$H(X) = H(\bar{X}), \quad \bar{X} = \text{complement of } X, \quad (10c)$$

$$H(X) \geq H(X^*) \quad (10d)$$

where X^* is the sharpened (intensified) version of X such that

$$\mu_{X^*}(x_{mn}) \geq \mu_X(x_{mn}) \quad \text{if } \mu_X(x_{mn}) \geq 0.5 \quad (11a)$$
$$\leq \mu_X(x_{mn}) \quad \text{if } \mu_X(x_{mn}) \leq 0.5. \quad (11b)$$

It is thus seen from property (10d) that the entropy of an image X increases/decreases with decrease/increase in contrast on X^*. Details with various applications are available in [3, 5].

5. Results

To study the effect of the transformation (from discrete grey value to corresponding intensity value) on the HVS based thresholding, the S^{-1} function (eq.(7)) was applied on different images such as Lincoln, Boy, Chromosome and Biplane which have multimodal, unimodal and bimodal histograms. It is assumed that the nature of transformation between discrete intensity and the corresponding grey value is very similar to that of Figure 2. The original input images and corresponding histograms are shown in Figures 4–7. The various transformed versions of the input images together with

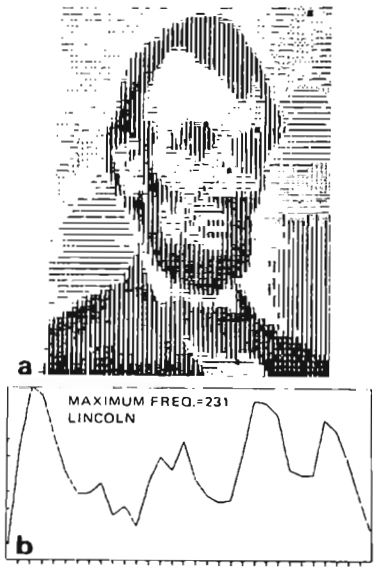

Figure 4. (a) Lincoln image. (b) Histogram.

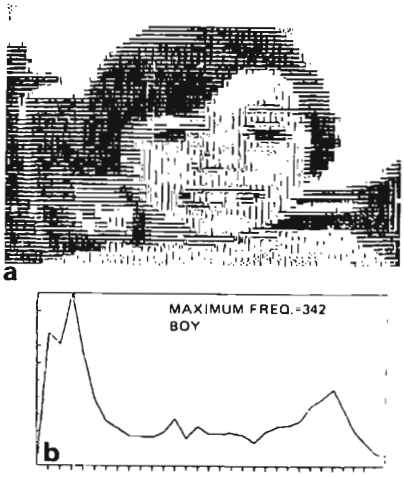

Figure 5. (a) Boy image. (b) Histogram.

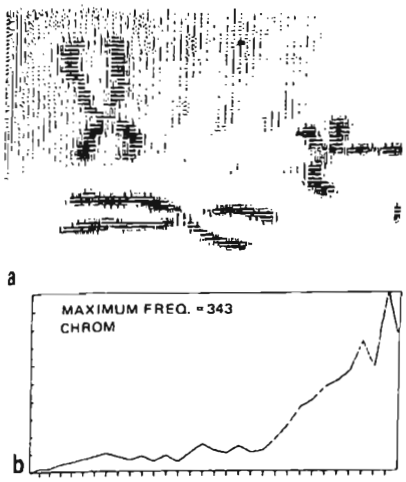

Figure 6. (a) Chromosome image. (b) Histogram.

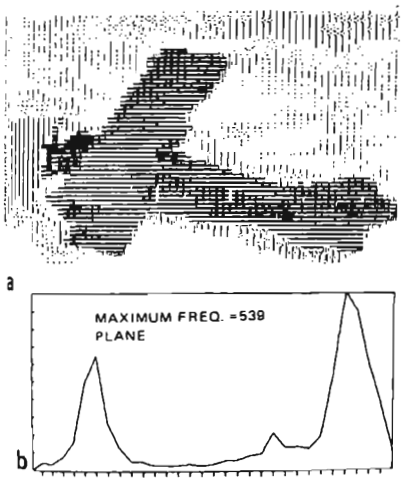

Figure 7. (a) Biplane image. (b) Histogram.

their histograms for different values of F_d (as an illustration, results corresponding to $F_d = 18$, 20 and 22 are considered) of eq. (7) are shown in Figures 8–11.

The program was simulated on a PDP-11/24 minicomputer system. The dot matrix printer was used to produce hard copy image output which represents various grey levels of the image with different graphic patterns. The 'Fuzzy Entropy' $H(x)$ of both original and transformed images were computed using eq. (8) and corresponding values are shown in Table 1.

Here the membership function, denoting bright image, is computed by Zadeh's S-function which is defined as

$$\begin{aligned}
\mu_X(x_{mn}) &= 0, && x_{mn} \le a,\\
&= 2\left(\frac{x_{mn}-a}{c-a}\right)^2, && a \le x_{mn} \le b,\\
&= 1 - 2\left(\frac{x_{mn}-c}{c-a}\right)^2, && b \le x_{mn} \le c,\\
&= 1 && x_{mn} \ge c \qquad (12)
\end{aligned}$$

where

$$a = l_{min}, \quad c = l_{max}, \quad b = \frac{a+c}{2}.$$

l_{min} and l_{max} denote minimum and maximum level respectively of the image.

From Table 1 it is seen that the $H(X)$ values of the transformed images are always greater than that of the original form. This implies that the S^{-1} function (eq.(7)) results in loss of overall contrast of the input images. The increase in $H(X)$ (or loss in contrast) is seen to be minimum for $F_d = 22$. This has (as mentioned in Section 3) also been reflected in the transformed histograms which are seen to have decrease in dynamic range with decrease in F_d value. As a result, the different regions of an input image tend to be closer, thus making some of the intermediate clusters finally shifted and merged. Furthermore, because of the relatively sharp variation at the ends of the transformation function (especially for $F_d = 18$ in Figure 3), some of the levels in the transformed histograms are found to be missing at either end.

The effect of grey level to intensity domain trans-

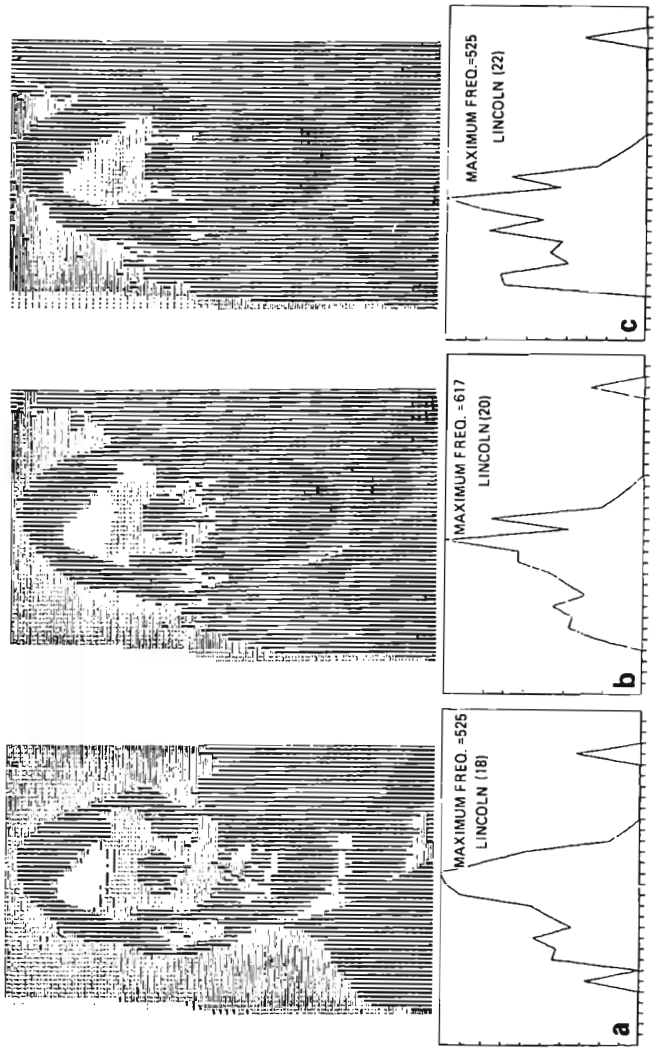

Figure 8. S^{-1} transformed Lincoln image and its histogram. (a) $F_a = 18$, (b) $F_a = 20$, (c) $F_a = 22$.

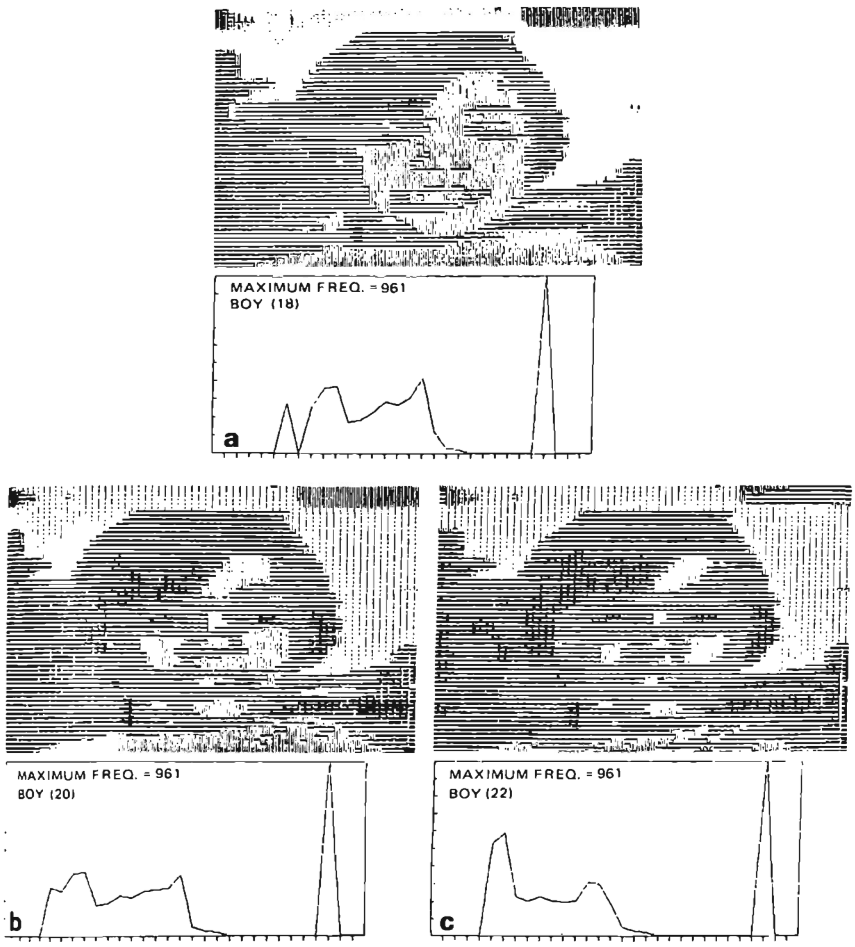

Figure 9. S^{-1} transformed Boy image and its histogram. (a) $F_d = 18$, (b) $F_d = 20$, (c) $F_d = 22$.

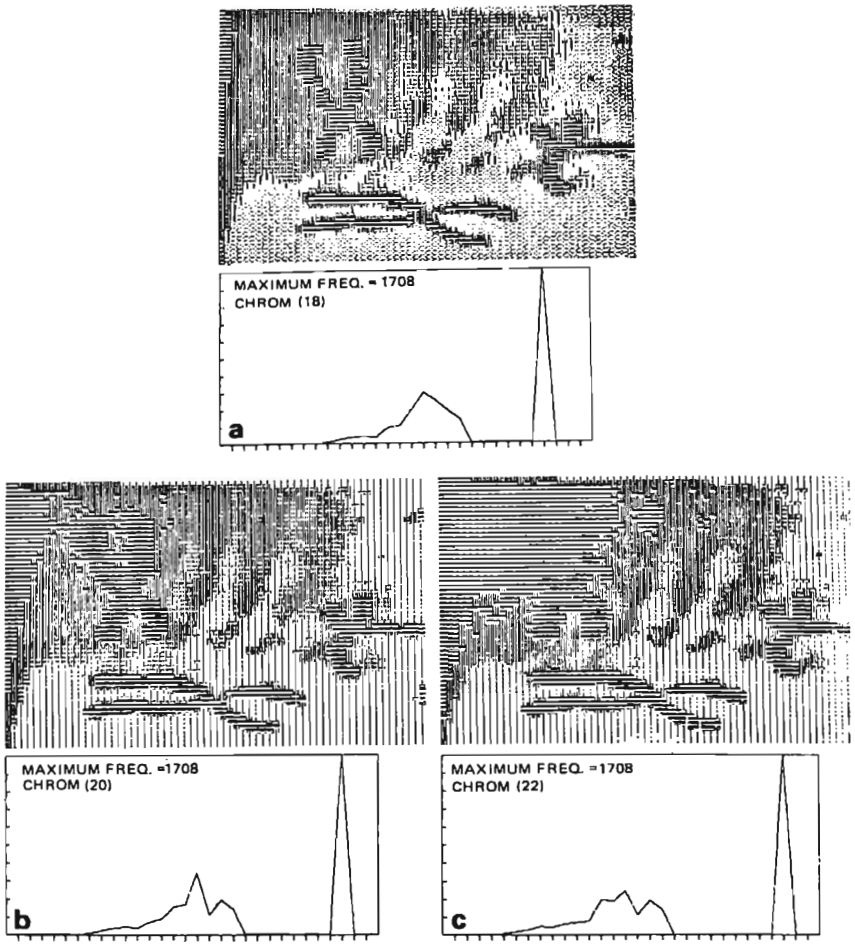

Figure 10. S^{-1} transformed Chromosome image and its histogram. (a) $F_d = 18$, (b) $F_d = 20$, (c) $F_d = 22$.

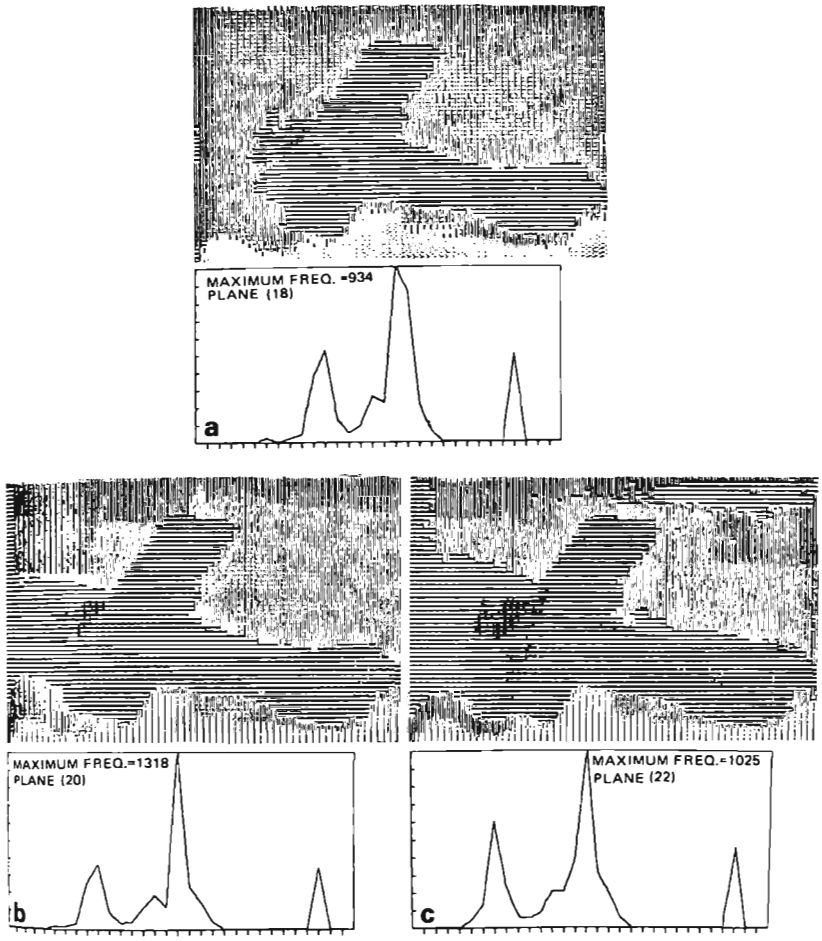

Figure 11. S^{-1} transformed Biplane image and its histogram. (a) $F_d = 18$, (b) $F_d = 20$, (c) $F_d = 22$.

Table 1
Entropy of images

Image	Entropy					
	Original	Transformed				
		$F_d = 18$	$F_d = 19$	$F_d = 20$	$F_d = 21$	$F_d = 22$
Lincoln	0.4816	0.8195	0.7804	0.7337	0.6903	0.6474
Coded Boy	0.3105	0.6492	0.6085	0.5574	0.5145	0.4818
Chromosome	0.2255	0.6563	0.6504	0.6034	0.5994	0.5871
Biplane	0.3047	0.8202	0.8071	0.7654	0.7388	0.7088

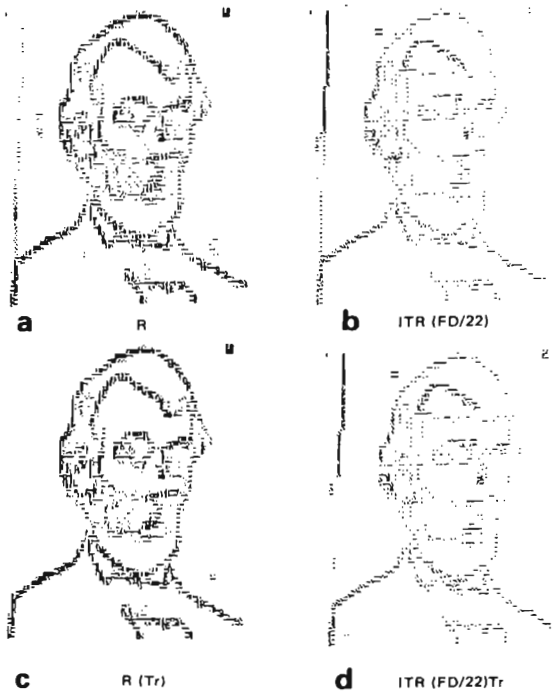

Figure 12. (a) Robert gradient edges of Figure 4(a). (b) HVS thresholded edges of Figure 4(a). (c) Robert gradient edges of Figure 8(c). (d) HVS thresholded edges of Figure 8(c).

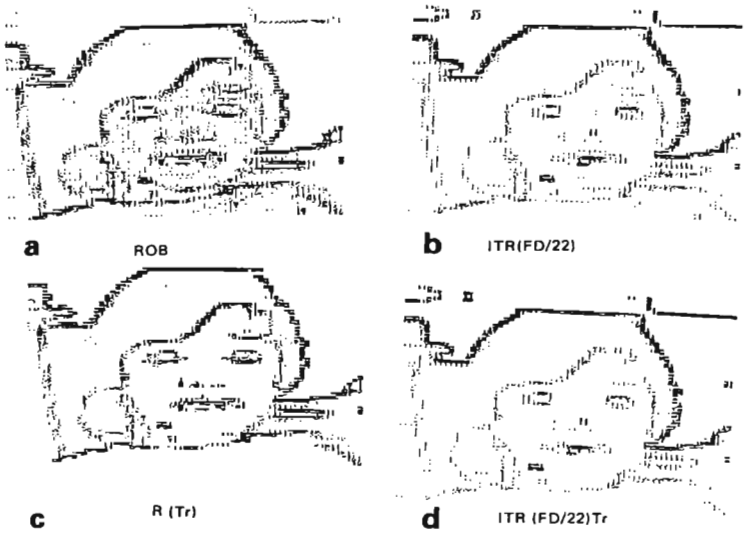

Figure 13. (a) Robert gradient edges of Figure 5(a). (b) HVS thresholded edges of Figure 5(a). (c) Robert gradient edges of Figure 9(c). (d) HVS thresholded edges of Figure 9(c).

rmation on the HVS based edge detection is demstrated through Figures 12–15 when both original images and their transformed versions are nsidered separately as input. As an illustration, effect only on the transformed images corresponding to $F_d = 22$ is shown here. The figures rresponding to part (a) represent Robert gradient age of the original images and those of part (b) w their significant edges extracted by HVS resholding (eq. (3)). Parts (c) and (d) on the other and correspond to transformed images (intensity omain) for $F_d = 22$. The parameters considered for VS thresholding are the same as in [1].

For Lincoln and Boy images, it is seen that the dges of Figures 12(d) and 13(d) (for transformed ages) are more thinned as compared to those of Figures 12(b) and 13(b) and have lost some of the formation. This is because of the fact that, the ransformed images have less dynamic range and onsequently the weak edges due to the weak level differences in the original images are no more present here. In case of the Biplane and Chromosome images, the picture is to some extent different. Here the transformed images possessed some additional overlapping regions because of splitting and merging of clusters in the original image. These additional regions generated some undesirable edges (Figures 14(d) and 16(d)) in addition to losing some significant edges.

6. Conclusion

The effect of grey level–intensity transformation on HVS based edge detection is investigated. A typical form of such transformation as mentioned by Pratt [2] is simulated here by a family of S^{-1}-type functions with varying slopes. The effect is investigated on a set of images having unimodal, bimodal and multimodal histograms.

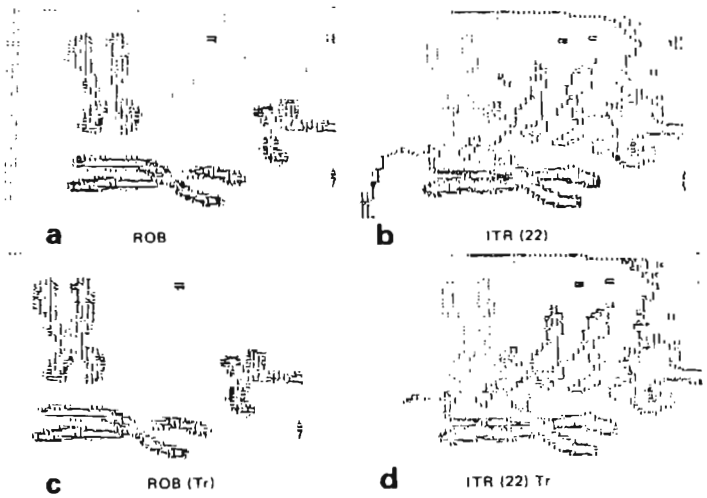

Figure 14. (a) Robert gradient edges of Figure 6(a). (b) HVS thresholded edges of Figure 6(a). (c) Robert gradient edges of Figure 10(c). (d) HVS thresholded edges of Figure 10(c).

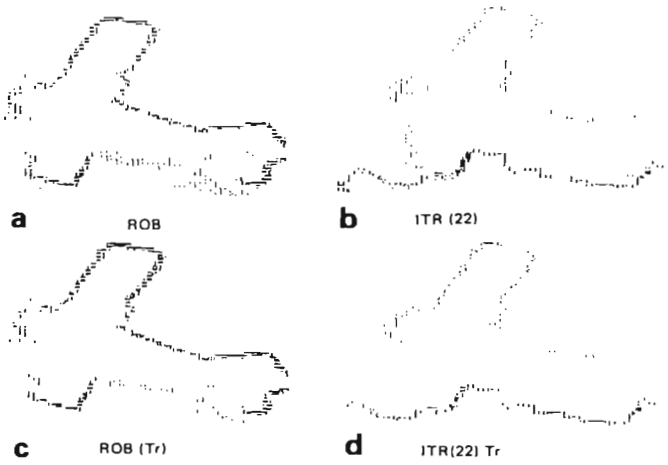

Figure 15. (a) Robert gradient edges of Figure 7(a). (b) HVS thresholded edges of Figure 7(a). (c) Robert gradient edges of Figure 11(c). (d) HVS thresholded edges of Figure 11(c).

The transformed intensity domain is found to have reduction in dynamic range, some unoccupied intensity levels and some undesirable regions because of splitting and merging of clusters of the original image. This is what is reflected in their entropy measures which are found to be greater than that of the original image. The final edge detected outputs thus do not seem (especially for Chromosome and Biplane images) to be encouraging.

This is probably because of the fact that the mapping functions used during transformation from discrete intensity levels to discrete grey levels were markedly different from the widely used S-type transformation [2] function for quality enhancement. So when S^{-1} type transformation (which is not appropriate here) was used to recover the discrete intensity levels, it gave rise to undesirable effects. Because it tends to split the levels around the higher and lower ends of the dynamic range and at the same time merges the levels at the middle range. As a result, spurious undesirable edges appear during the edge extraction procedure. Furthermore, the error due to digitization, round-off and inherent nonlinearity of the device makes it difficult to get back the original luminance values [2].

Acknowledgement

The authors gratefully acknowledge Professor D. Dutta Majumder for his interest in this work and Mr. N. Chatterjee for typing the manuscript.

References

[1] Kundu, M.K. and S.K. Pal (1986). Thresholding for edge detection using human psychovisual phenomena. *Patt. Recog. Lett.* 4, 433–441.

[2] Pratt, W.K. (1978). *Digital Image Processing*. Wiley Interscience, New York, 447–457.

[3] Pal, S.K. and R.A. King (1981). Image enhancement using smoothing with fuzzy sets. *IEEE Trans. Syst. Man Cybernet.* 11, 494–501.

[4] De Luca, A. and S. Termini (1972). A definition of nonprobabilistic entropy in setting of fuzzy set theory. *Inform. and Control* 20, 301–312.

[5] Pal, S.K. (1982). A note on the quantitative measure of image enhancement through fuzziness. *IEEE Trans. Patt. Anal. Machine Intell.* 4, 204–208.

[6] Zadeh, L.A. (1975). Calculus of fuzzy restriction. In: L.A. Zadeh et al., Eds., *Fuzzy Sets and their Applications to Cognitive and Decision Processes*. Academic Press, London, 1–39.